physica status solidi a
www.pss-a.com

Check for updates

Ultrawide Bandgap Channel Polarization-Doped Junction Field-Effect Transistor

Madhav Ramesh, Shivali Agrawal, Huili Grace Xing, and Debdeep Jena*

An ultrawide bandgap (UWBG) AlGaN channel polarization-doped junction field-effect transistor (POLJFET) grown by molecular beam epitaxy on a bulk AlN substrate is presented. The POLJFET leverages distributed polarization doping for the *p*-side gate, owing to the challenges associated with reliable acceptor impurity doping in UWBG AlGaN. Successful gate control of the transistor channel by pn junction field effect, with a threshold voltage of ≈ -30 V, is demonstrated. The transistor shows a significantly low OFF current (<10 nA mm^{-1}) while the ON current is 0.03 mA mm^{-1}, primarily limited by the high contact resistivity of the n-type AlGaN channel. This is expected due to the low doping of n-AlGaN by design and can be mitigated by contact optimization techniques (either by regrowth or ion implantation) in future iterations.

1. Introduction

Semiconductor devices using ultrawide bandgap (UWBG) Al(Ga)N have the potential to go beyond the current power electronics limitations posed by the properties of GaN and SiC. The large critical electric field (up to 15.4 MV cm^{-1} in AlN)—and therefore a high Baliga's Figure of Merit—makes it an excellent contender for power electronic switching device applications.[1] Junction field-effect transistors (JFETs) allow high breakdown voltage operation and low gate leakage[2] by utilizing the entire energy bandgap of pn diodes compared to a part of the bandgap of Schottky barriers. There exists the possibility of enhancement-mode (E-mode) operation provided the layer thicknesses, compositions, and doping are selected carefully to account for trade-offs between ON current, breakdown voltage, and threshold voltage. Fin and dual-gated geometries also enable this possibility.[3,4] In addition, the mechanism of JFETs, unlike metal-semiconductor field-effect transistors (MESFETs), does not rely on the metal-semiconductor interface which is known to degrade at high temperatures, thereby resulting in superior thermal stability.[5] A significant challenge in realizing UWBG AlGaN *p*-type layers is the acceptor doping. Magnesium, the common acceptor for GaN has an activation energy $E_a \approx 200$ meV for GaN,[6] but $E_a \approx 630$ meV for AlN,[7] precluding its room temperature usage in high-Al-content AlGaN, making an UWBG pn junction gate of a desired JFET impractical by acceptor doping.

The large tunable bandgap of AlGaN combined with its spontaneous and piezoelectric polarization enables distributed polarization doping (DPD) by grading the AlGaN layer to form a 3D hole gas, eliminating the need for acceptor doping.[8] Recently, this technique was used to realize pn diode structures.[9,10] This opens the possibility of realizing polarization-doped junction field-effect transistors (POLJFETs) first proposed in ref. [11], where a DPD pn junction gate replaces the Schottky gate of the POLFETs.[12–14] In addition, epitaxial growth on a single-crystal AlN substrate ensures high quality of the device structure.[15] Here, we report the first realization of a UWBG $Al_{0.8}Ga_{0.2}N$ POLJFET grown on a bulk AlN substrate, with a DPD *p*-gate layer.

2. Experimental Section

The POLJFET semiconductor layer structure shown in **Figure 1**a was grown by plasma assisted molecular beam epitaxy (MBE) on an Al polar single-crystal bulk AlN substrate. A 150 nm $Al_{0.8}Ga_{0.2}N$ channel with $N_d \approx 10^{18}$ cm^{-3} silicon doping was grown on a $\approx$500 nm undoped AlN buffer layer. A $t_\pi = 75$ nm compositionally graded AlGaN layer was then grown by varying the Al mole fraction from $x_1 \approx 80\% \rightarrow x_2 \approx 15\%$ along the growth direction, followed by a 10 nm heavily magnesium-doped *p*-GaN gap layer to form the *p*-ohmic gate contact. Figure 1c shows hexagonal cracks due to relaxation. X-Ray diffraction spectra shown in Figure 1d confirmed the compositional grading of the DPD layer. POLJFETs, as shown in Figure 1a, were fabricated by inductively coupled plasma reactive ion etching (ICP-RIE) etching down $\approx$90 nm to access the n-AlGaN channel layer. A subsequent $\approx$260 nm deep ICP-RIE etch was performed down to the AlN buffer layer for device isolation. The etched features are evident in the scanning electron microscope (SEM) image in

M. Ramesh, H. G. Xing, D. Jena
School of Electrical and Computer Engineering
Cornell University
Ithaca, NY 14853, USA
E-mail: mr974@cornell.edu

S. Agrawal
Department of Chemical and Biomolecular Engineering
Cornell University
Ithaca, NY 14853, USA

H. G. Xing, D. Jena
Department of Materials Science and Engineering
Cornell University
Ithaca, NY 14853, USA

The ORCID identification number(s) for the author(s) of this article can be found under https://doi.org/10.1002/pssa.202401023.

DOI: 10.1002/pssa.202401023

 © 2025 Wiley-VCH GmbH

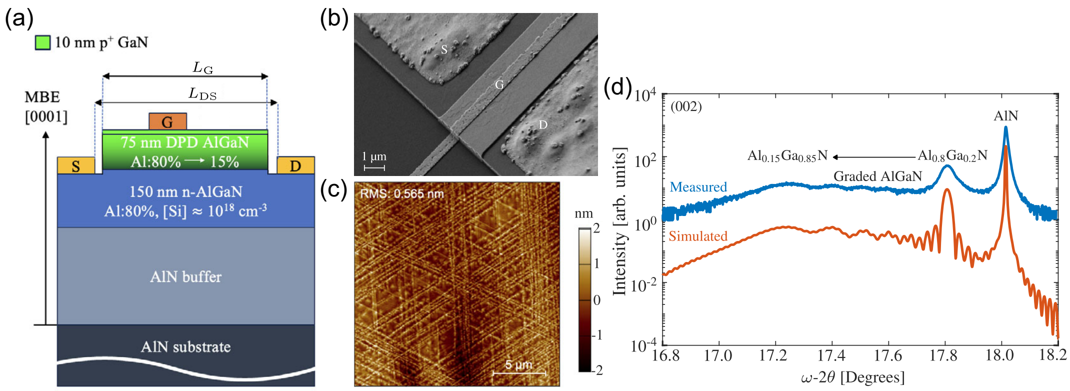

Figure 1. a) Cross-sectional view of the POLJFET. b) SEM image indicating gate, source, and drain terminals of the transistor. c) Atomic force microscopic image of the sample surface prior to processing. Strain relaxation of the structure is observed through long crack lines forming on the surface that cross each other at 60 or 120°. d) Measured and simulated ω-2θ X-Ray diffraction scan across the (002) peak.

Figure 1b, which also indicates the gate, source, and drain regions of the fabricated device. V/Al/Ni/Au (15/80/40/100 nm) stack contacts were deposited by E-beam evaporation and annealed in N_2 ambient at 800 °C for 30 s for source/drain metallization. $L_G = 4\,\mu m$ and $L_G = 5\,\mu m$ gate regions and source-to-drain distances $L_{DS} = 6\,\mu m$ and $L_{DS} = 7\,\mu m$, respectively, were defined by optical photolithography. And, 15/20 nm Ni/Au *p*-gate Ohmics were formed by 450 °C annealing in O_2 ambient for 60 s.

Figure 2a shows the calculated energy band diagram and carrier density under the gate of the POLJFET at equilibrium. A high hole concentration in the DPD layer, combined with the lower n-type doping, indicated a one-sided p^+/n junction, with most of the depletion region in the n-doped side. The mobile hole density in the DPD layer was estimated to be

$$p_\pi = \frac{dP}{dz} \approx \frac{P(x_1) - P(x_2)}{t_\pi} \approx 3 \times 10^{18}\ \text{cm}^{-3} \tag{1}$$

where $P(x_1)$ and $P(x_2)$ are the polarization values at Al compositions x_1 and x_2 respectively, and t_π is the thickness of the graded AlGaN layer. The n-AlGaN layer with $10^{18}\ \text{cm}^{-3}$ Si donor doping was estimated to have a mobile electron concentration $\approx 4.5 \times 10^{17}\ \text{cm}^{-3}$ assuming a donor ionization energy of 50 meV.[16] This resulted in the formation of a p^+/n junction diode. It should be noted that the concentration of holes could be controlled by varying the thickness of the DPD layer along with appropriate compositional and strain engineering.

Temperature-dependent current–voltage (I–V) characteristics of the diode were measured using a Keysight B1505A Power Device Analyzer with a thermal chuck (ATT systems GmbH). The transistor characteristics were measured using a Keithley 4200 A semiconductor parameter analyzer. Figure 2b shows the measured two-terminal gate-source currents of a 5 μm gate length POLJFET for temperatures between 25 and 300 °C. The forward current was limited by Schottky-like source/drain contacts due to the relatively low doping and high Al content of the channel layer; this can be improved in the future. The gate-source pn diode current increased with temperature, flowing 10 A cm^{-2} at 300 °C, with a turn on near 3–5 V, and very low reverse leakage current.

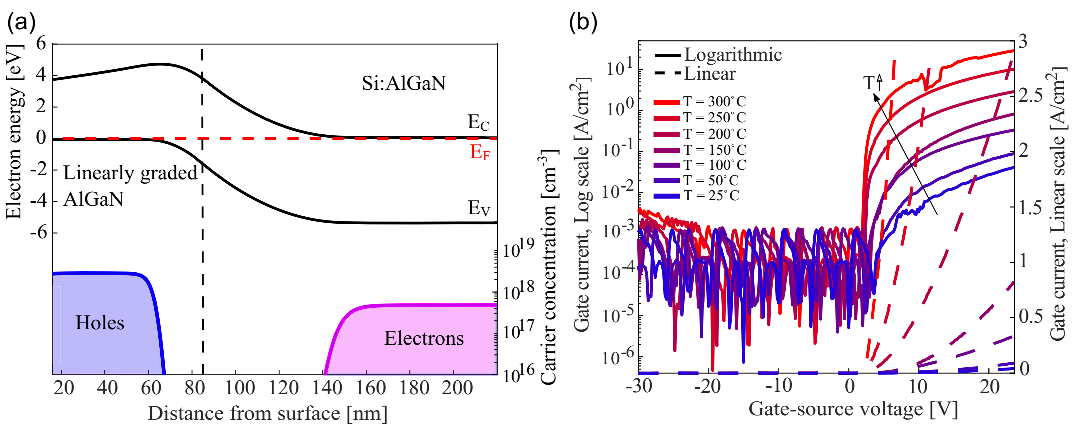

Figure 2. Characteristics of the pn junction gate. a) Energy band diagram and carrier density from solving 1D Poisson. b) Temperature-dependent *I–V* characteristics between the gate and the source of a transistor with $L_G = 5\,\mu m$. The forward bias current increases with temperature, as expected from diode theory.

© 2025 Wiley-VCH GmbH

18626319, 0, Downloaded from https://onlinelibrary.wiley.com/doi/10.1002/pssa.202401023 by Cornell University, Wiley Online Library on [08/05/2025]. See the Terms and Conditions (https://onlinelibrary.wiley.com/terms-and-conditions) on Wiley Online Library for rules of use; OA articles are governed by the applicable Creative Commons License

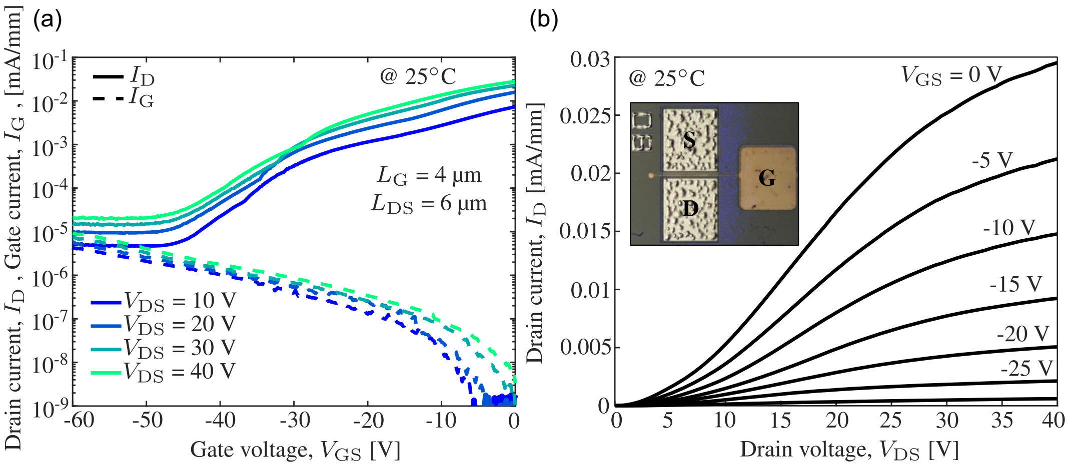

Figure 3. Transistor electrical characteristics for $L_G = 4$ μm at room temperature. a) Transfer curves indicating drain current modulation via the gate over three orders of magnitude. b) Output characteristics at various gate voltages. Inset: optical image of the POLJFET measured in (a) and (b).

The POLJFET works by modulating the conductive layer thickness of the n-channel by depletion from the reverse-biased DPD p^+/n junction. By design, the doping of the n-AlGaN layer ($N_d \approx 10^{18}$ cm^{-3} resulting in $\approx 4.5 \times 10^{17}$ cm^{-3} mobile electrons) was chosen to be much lower than that of the *p*-DPD layer hole concentration ($p_\pi \approx 3 \times 10^{18}$ cm^{-3}). This was due to the fact that the n-channel was required to be depleted by the gate with minimal depletion of the *p*-DPD layer. **Figure 3**a shows the measured transfer characteristics of a POLJFET of dimensions shown in the figure for various drain bias voltages. The decrease of channel current for larger reverse bias of the gate DPD p^+/n junction confirmed that the current was modulated by junction field effect with a threshold voltage of ≈ -30 V. This indicated the first successful operation of a POLJFET with a UWBG AlGaN channel with a DPD p^+/n junction gate. But the ON current of the transistor was only ≈ 0.03 mA mm^{-1} at 40 V drain bias. The gate leakage current was significantly low (<10 nA mm^{-1}) throughout the measurement, which is characteristic of the UWBG reverse-biased pn junction. Figure 3b shows the output characteristics of the POLJFET, with a microscope image of the device shown in the inset. Gate control of the POLJFET was observed, but the poor n-channel contacts were evident in the Schottky like turn on, which limited the current drive to several orders lower than what was possible in a future iteration with better contacts.

3. Conclusion

In conclusion, we have demonstrated a UWBG channel POLJFET grown by MBE on a bulk AlN substrate. Successful gate control of the n-type AlGaN channel by junction field effect is observed. Temperature-dependent measurements of the pn junction gate suggests carrier ionization with increasing temperature. The OFF state of the transistor shows very low current (<10 nA mm^{-1}), and the ON state current can further be improved through source–drain contact optimization in the future: either by regrowth or ion implantation. Demonstration of the POLJFET operation opens a new design pathway for power electronics devices based on aluminum nitride, making it possible to leverage its desirable electronic properties.

Supporting Information

Supporting Information is available from the Wiley Online Library or from the author.

Acknowledgements

This work was supported in part by the Ultra Materials for a Resilient Energy Grid (epitaxy), an Energy Frontier Research Center funded by the U.S. Department of Energy, Office of Science, Basic Energy Sciences under Award #DE-SC0021230, in part by ARO Grant #W911NF2220177 (device fabrication), and in part by DARPA UWBGS Sponsor Contract HR0011470637/HR0011472427 (characterization). This work was performed in part at the Cornell NanoScale Facility (an NNCI member supported by NSF Grant NNCI-2025233).

Conflict of Interest

The authors declare no conflict of interest.

Data Availability Statement

The data that support the findings of this study are available from the corresponding author upon reasonable request.

Keywords

distributed polarization doping, junction field-effect transistors, ultrawide bandgap AlGaN

Received: December 27, 2024
Revised: March 23, 2025
Published online:

© 2025 Wiley-VCH GmbH

18626319, 0, Downloaded from https://onlinelibrary.wiley.com/doi/10.1002/pssa.202401023 by Cornell University, Wiley Online Library on [08/05/2025]. See the Terms and Conditions (https://onlinelibrary.wiley.com/terms-and-conditions) on Wiley Online Library for rules of use; OA articles are governed by the applicable Creative Commons License

[1] J. Y. Tsao, S. Chowdhury, M. A. Hollis, D. Jena, N. M. Johnson, K. A. Jones, R. J. Kaplar, S. Rajan, C. G. Van de Walle, E. Bellotti, C. L. Chua, R. Collazo, M. E. Coltrin, J. A. Cooper, K. R. Evans, S. Graham, T. A. Grotjohn, E. R. Heller, M. Higashiwaki, M. S. Islam, P. W. Juodawlkis, M. A. Khan, A. D. Koehler, J. H. Leach, U. K. Mishra, R. J. Nemanich, R. C. N. Pilawa-Podgurski, J. B. Shealy, Z. Sitar, M. J. Tadjer, et al., *Adv. Electron. Mater.* **2018**, *4*, 1600501.

[2] M. Shatalov, G. Simin, J. Zhang, V. Adivarahan, A. Koudymov, R. Pachipulusu, M. Asif Khan, *IEEE Electron Device Lett.* **2002**, *23*, 452.

[3] R. Zhang, J. Liu, Q. Li, S. Pidaparthi, A. Edwards, C. Drowley, Y. Zhang, *IEEE Trans. Power Electron.* **2021**, *37*, 6253.

[4] M. Kaneko, M. Nakajima, Q. Jin, T. Kimoto, *IEEE Electron Device Lett.* **2022**, *43*, 997.

[5] J. C. Zolper, *Solid-State Electron.* **1998**, *42*, 2153.

[6] S. Brochen, J. Brault, S. Chenot, A. Dussaigne, M. Leroux, B. Damilano, *Appl. Phys. Lett.* **2013**, *103*, 032102.

[7] Y. Taniyasu, M. Kasu, T. Makimoto, *Nature* **2006**, *441*, 325.

[8] J. Simon, V. Protasenko, C. Lian, H. Xing, D. Jena, *Science* **2010**, *327*, 60.

[9] S. Agrawal, L. van Deurzen, J. Encomendero, J. E. Dill, H. W. (Sheena) Huang, V. Protasenko, H. G. Xing, D. Jena, *Appl. Phys. Lett.* **2024**, *124*, 102109.

[10] T. Kumabe, A. Yoshikawa, M. Kushimoto, Y. Honda, M. Arai, J. Suda, H. Amano, in *2023 Int. Electron Devices Meeting (IEDM)*, IEEE **2023**, pp. 1–4.

[11] D. Jena, *Ph.D. Thesis*, University of California, Santa Barbara **2003**.

[12] S. Rajan, H. Xing, S. DenBaars, U. K. Mishra, D. Jena, *Appl. Phys. Lett.* **2004**, *84*, 1591.

[13] A. M. Armstrong, B. A. Klein, A. Colon, A. A. Allerman, E. A. Douglas, A. G. Baca, T. R. Fortune, V. M. Abate, S. Bajaj, S. Rajan, *Jpn. J. Appl. Phys.* **2018**, *57*, 074103.

[14] J. Lemettinen, N. Chowdhury, H. Okumura, I. Kim, S. Suihkonen, T. Palacios, *IEEE Electron Device Lett.* **2019**, *40*, 1245.

[15] Z. Zhang, J. Encomendero, R. Chaudhuri, Y. Cho, V. Protasenko, K. Nomoto, K. Lee, M. Toita, H. G. Xing, D. Jena, *Appl. Phys. Lett.* **2021**, *119*, 162104.

[16] J. H. Park, D. Y. Kim, E. F. Schubert, J. Cho, J. K. Kim, *ACS Energy Lett.* **2018**, *3*, 655.

© 2025 Wiley-VCH GmbH

18626319, 0, Downloaded from https://onlinelibrary.wiley.com/doi/10.1002/pssa.202401023 by Cornell University, Wiley Online Library on [08/05/2025]. See the Terms and Conditions (https://onlinelibrary.wiley.com/terms-and-conditions) on Wiley Online Library for rules of use; OA articles are governed by the applicable Creative Commons License